Contents lists available at ScienceDirect

Dyes and Pigments

journal homepage: http://ees.elsevier.com

Steric hindrances and spectral distributions affecting energy transfer rate: A comparative study on specifically designed donor-acceptor pairs

E. Domenichini [a], S. Doria [b,*], M. Di Donato [b,c], L. Cupellini [d], G. Biagiotti [e,**], A. Iagatti [b], L. Bussotti [b], B. Mennucci [d], S. Cicchi [e], P. Foggi [b,c,f,g]

[a] University of Strasbourg, IPCMS, 23 Rue Du Loess, 67034, Strasbourg, France
[b] European Laboratory for Non Linear Spectroscopy (LENS), Universita' Degli Studi di Firenze, Via Nello Carrara 1, 50019, Sesto Fiorentino, Florence, Italy
[c] CNR-ICCOM, Consiglio Nazionale Delle Ricerche-Istituto-Istituto di Chimica Dei Composti OrganoMetallici, Via Madonna Del Piano 10, 50019, Sesto Fiorentino, Firenze, Italy
[d] Dipartimento di Chimica e Chimica Industriale, Università di Pisa, Via G. Moruzzi 13, 56124, Pisa, Italy
[e] Dipartimento di Chimica ''Ugo Schiff'', Università Degli Studi di Firenze, Via Della Lastruccia, 3-13, 50019, Sesto Fiorentino, Florence, Italy
[f] CNR-INO, Consiglio Nazionale Delle Ricerche – Istituto Nazionale di Ottica, Largo Fermi 6, 50125, Florence, Italy
[g] Dipartimento di Chimica, Biologia e Biotecnologie, Università di Perugia, Via Elce di Sotto 8, 06100, Perugia, Italy

ABSTRACT

In this work the photophysics of four bichromophoric units was studied by means of static and time resolved spectroscopy, with the aim of disentangling the contribution of steric and electronic factors in regulating the efficiency of electronic energy transfer (EET). The newly synthesized dyads share the same acceptor moiety, a substituted BODIPY chromophore, and differ either in the donor or in the molecular bridge connecting the two units. The use of different linkers allows for tuning the conformational flexibility of the dyad, while changing the donor has an influence on the electronic coupling and spectral overlap between the two chromophores. The efficiency of energy transfer is extremely high in all the four dyads and can be modelled within the frame of the Förster equation. In the special case of a dimeric donor, a theoretical analysis was performed to further support the experimental findings. Geometry optimization at DFT level indicated that different conformations with similar energy can exist in solution, explaining the observed multi-exponential EET. Furthermore, energy transfer rates, computed at DFT level, resulted in optimal agreement with the experimental ones. Our analysis allowed to conclude that, in case of the studied systems, steric hindrance and donor-acceptor relative orientations plays a prominent role in regulating the EET dynamics, even overcoming electronic effects.

1. Introduction

Energy transfer processes have been widely investigated in the last decades, especially because of their fundamental importance in photosynthesis [1]. A deep comprehension of the factors regulating the efficiency and kinetics of energy transfer is however also important for the development of artificial light-harvesting materials to be used for light energy conversion [2–7]. To make one step forward in the comprehension of energy transfer mechanisms, one of the most valued approaches is to reduce the complexity of the system by studying single pairs of donor-acceptor moieties, synthesized on purpose to have the desired electronic and spectral properties, in addition to specific conformations.

The full comprehension of the overall energy transfer processes involves the identification of the energy pathways in the molecular system and the elucidation of the involved timescale. Ultrafast pump-probe techniques are a perfect tool to investigate excited state dynamics and energy transfer processes from the sub-picosecond up to the nanosecond time-scale [8–11], providing the necessary spectral and temporal resolution to identify the nature of intermediate and final states and to characterize the temporal regimes of the energy flow. In this work, we synthesized and characterized the photophysical behaviour of three dyads, studying them in different solvents both by stationary and transient absorption spectroscopy. The spectroscopic measurements, supported by a theoretical analysis, allowed us to obtain a quantitative estimate of the transfer rate and to infer the donor-acceptor effective distance by applying the Förster theory.

The three dyads under investigation are characterized by the same acceptor moiety, consisting in a modified BF 2-chelated dipyrromethene compounds, known also as BODIPY. Recently these molecules have been considerably studied in literature, because of

* Corresponding author.
** Corresponding author.
E-mail addresses: doria@lens.unifi.it (S. Doria); giacomo.biagiotti@unifi.it (G. Biagiotti)

https://doi.org/10.1016/j.dyepig.2019.108010
Received 7 October 2019; Received in revised form 26 October 2019; Accepted 30 October 2019
Available online xxx
0143-7208/

their outstanding photo-physical properties, such as large molar extinction coefficients and high fluorescence quantum yield (QY) [12].

Furthermore, chemical modifications of the core substituents allow fine tuning of their spectral and electronic properties, making also possible to obtain chromophores with far-red absorption and emission. For these reasons, BODIPY-based materials have found wide-spread applications, ranging from fluorescent probes for biosensors [13–16], to antenna in dye-sensitized solar cells [17–19]. The acceptor molecule studied in this work consists in a BODIPY core with two styryl groups attached in the alpha positions and one phenyl group in the meso position (Fig. S1a in S.I.). This chemical modification to the BODIPY core significantly shifts the absorption spectrum toward the red region respect to the unmodified analogue, from 500 to 620 nm.

In a previous publication [20] we investigated the dynamics and efficiency of electronic energy transfer (EET) in a molecular dyad composed of the same BODIPY acceptor and an Aminostyrylpyridinium donor (compounds D in Fig. 1), linked together via a covalent non-conjugated bridge, which infers conformational flexibility to the dyad, allowing multiple relative orientations of the two units. Aminostyrylpyridinium dyes are known in scientific literature to show a charge transfer state due to electron density separation between the dimetylamino group and the pyridinium moiety, which causes cis-trans isomerization [21–27]. These dyes have found several application as well, as sensitizers in photographic industry, laser dyes, additives in bio-sensors [21,22]. In Ref. [20], by combining transient absorption experiments and a theoretical analysis at the M062X/6-311G(d)/PCM level we found different stable configurations of the dimer, resulting in multiple EET rates. The theoretical estimate of energy transfer time constants, based on the calculation of the electronic coupling for the different conformers and the application of the Förster expression, retrieved EET rates well in agreement with the experimental ones. The results showed that a few relative orientations between donor and acceptor dipoles mainly contributed to the observed energy transfer kinetics. Starting from these previous results, in order to further understand of the role played by different factors in determining the energy transfer rate, here we synthesized different dyads which shared the same acceptor chromophore of previously analysed system, but either a different donor or a different linker between donor and acceptor.

We repeated the previous characterization for the newly synthesized systems, both at the experimental and theoretical level. Once again, a conformational analysis at DFT level allowed to identify the most stable conformers and give a theoretical estimate of the EET rates. The comparison between experimental and theoretical results obtained for the new dyads and the previously analysed one allowed us to disentangle the influence of different molecular factors, such as the bridge flexibility or the nature of the donor chromophore, on the observed EET rates.

2. Materials and methods

2.1. Synthesis of the samples

All the reagents, whose synthesis is not described, were commercially available and have been used without any further purification, if not specified otherwise. The complete synthetic approach for the preparation of compounds 1, 2 and 3 is described in the Supporting Information section and schematized in Figs. S18, S17, S19.

Rf values are referred to TLC on silica gel plate (0.25 mm, Merck silica gel 60 F254). NMR spectra were recorded on Varian Gemini 200 MHz or Varian Mercury 400 MHz at room temperature. Chemical shifts were reported in parts per million (ppm) relative to the residual solvent peak rounded to the nearest 0.01 for proton and 0.1 for carbon (reference: CHCl3 [1H: 7.26,13 C: 77.0], DMSO [1H: 2.50,13 C: 39.7], MeOH [1H: 3.35,13 C: 49.3]. Coupling constants J were reported in Hz to the nearest 0.01 Hz. Peak multiplicity was indicated as follows: s (singlet), d (doublet), t (triplet), q (quartet), m (multiplet) and br (broad signal). IR spectra were recorded on a PerkinElmer FT-IR 881 or Shimadzu FT-IR 8400s or Shimadzu IRAffinity-1s spectrometer. IR data are reported as frequencies in wavenumbers (cm^{-1}). Mass spectra were recorded on a Thermoscientific LCQ-Fleet. UV–Vis spectra were recorded on Varian Cary 4000 Uv–vis spectrophotometer using 1 cm cell. Fluorescence spectra were registered on a Jasco FP750 spectrofluorimeter using 1 cm cell. Elemental analyses were performed with a Thermofinnigan CHN–S Flash E1112 analyser.

The chemical structure of the analysed dyads is shown in Fig. 1.

2.2. Transient absorption spectroscopy

Sub-picosecond transient absorption spectra (TAS) have been recorded using a previously described system [28].

The system is based on a Ti:sapphire regenerative amplifier laser system (BMI Alpha 1000) and fs-laser oscillator (Spectra Physics Tsunami). For the experiments described in this work, visible pump pulses have been obtained by pumping a home-made Travelling wave Optical Parametric Amplifier (TOPAS) with a portion of the

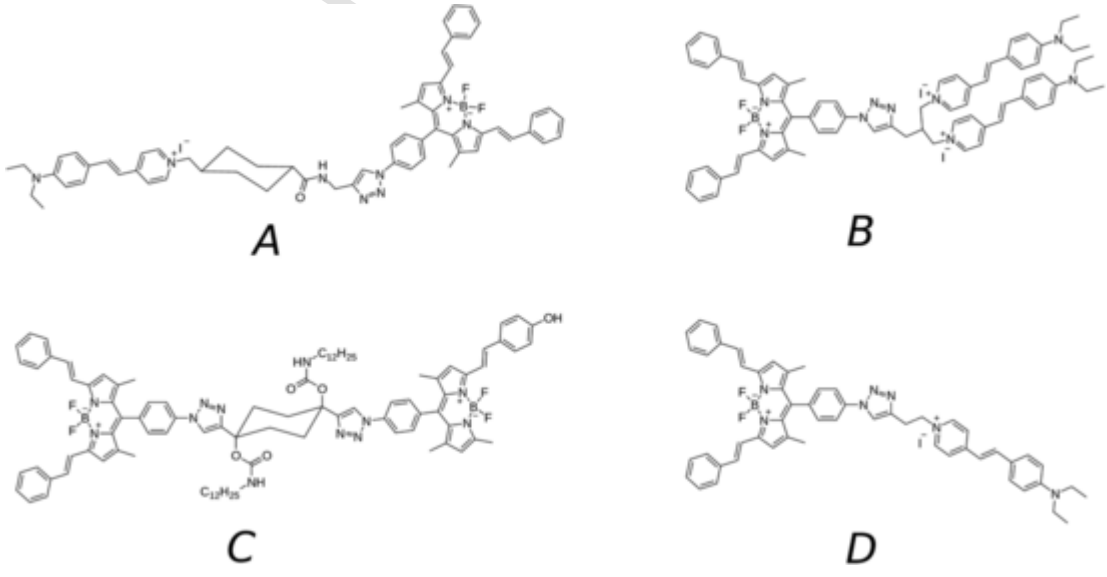

Fig. 1. Chemical structure of the compounds under investigation. Compound D has been studied in Ref. [20].

fundamental output. The excitation wavelength has been tuned in agreement with the optical absorption spectrum of the different dyads. Excitation power was set at 100–150 nJ. The white light continuum probe pulses have been obtained by focusing a portion of the 800 nm laser radiation on a 2 mm thick sapphire window. A part of the white light continuum has been split off using a beam splitter and used as reference signal. Pump-probe delays for a time interval spanning between −5 and 1500 ps were obtained by directing the probe beam through a motorized stage. After the sample, the probe beam was dispersed through a flat field monocromator and imaged on a home-made detector. The sample was contained in a quartz cell with a 2 mm optical path, mounted on a movable stage in order to minimize photodegradation. The collected kinetic traces have been analysed by a global analysis procedure [29]. A preliminary singular values decomposition (SVD) [30] allowed to estimate the number of kinetic components to be used for the fit. Global analysis has been performed using the GLOTARAN software (http://glotaran.org) [31,32], and employing a linear unidirectional kinetic scheme.

2.3. Computational methods

Following previous works [20,33,34], we used a (TD)DFT-based strategy to compute the excited states and the EET couplings between the two styrylpyridinium donor moieties and the BODIPY acceptor. EET couplings are computed with a well established perturbative approach as the interaction among the quantum mechanical transition densities of the isolated moieties [35,36]. The effects of the solvent (here, chloroform) were systematically included in all calculations through the integral equation formalism polarizable continuum model (IEFPCM) [37], which treats the solvent as a homogeneous dielectric medium, characterized by its static and optical dielectric constants. In particular, with IEFPCM it is possible to compute the explicit solvent contribution to the coupling, arising from the dielectric in which the donor and acceptor are embedded [36]. Geometry optimizations were carried out with the M06–2X [38] functional and the 6-311G(d) basis set, as in our previous work. Excited states and the corresponding EET couplings were computed with the long-range corrected CAM-B3LYP [39] functional in combination with the 6-311 + G (2d,p) basis set. Owing to the greater conformational complexity of dyad D, which presents several single bonds around which rotations are possible, a complete mapping of all conformations of the dyad is not possible. Instead, we selected three relevant dihedral angles (β/γ/δ) which were randomly varied to generate several conformations. After removing conformations with close contacts between atoms, we optimized the remaining structures at the DFT level. Redundant structures, which after the optimization had ended in the same minimum, were considered only once. For the final nine conformations, we computed the relative free energies at the M06–2X/6-311 + G (2d,p) level, including non-electrostatic contributions in the solvation free energy with the SMD solvent model [40]. The thermal contribution to the free energy was estimated through harmonic frequency calculations at the M06–2X/6-311G(d) level. Finally, electronic couplings were computed as described above, computing separately the coupling between each styrylpyridinium donor and the BODIPY acceptor.

EET rates. EET rates were computed from couplings assuming the validity of the Fermi Golden Rule

$$K_{EET} = \frac{2\pi}{h} V_{DA}^2 \times \mathrm{FCWD} \quad (1)$$

where V_{DA} represents the EET coupling, and *FCWD* is the Franck-Condon weighted density of states, which measures the energetic superposition between vibronic levels of the donor and acceptor. For EET involving bright excited states, the *FCWD* can be obtained directly from the spectral overlap of area-normalized donor emission and acceptor absorption [41]. The spectral overlap calculated for dyad B in chloroform is 290×10^{-6} cm, close to the value of 280×10^{-6} cm obtained for dyad D in Ref. [20].

3. Experimental results

The absorption spectra of all the samples under investigation (plus the molecule of ref. [20]) are reported in Fig. 1. The first dyad (A) consists in the same styryl-pyridinium donor and BODIPY acceptor studied in Ref. [20]; however, here the covalent bridge is a cyclohexane with long aliphatic chains substituents. This linker limits the conformational flexibility of the dyads, reducing the possible relative orientations of the two moieties, which in this case are kept at fixed relative distance.

In dyad B we used a donor consisting of a dimer of styrylpyridinium moieties. The purpose of this choice was to study the influence of both steric and electronic factors on the energy transfer. The donor-acceptor linker, being the same of ref. [20] was chosen to allow conformational mobility of the two units.

The last dyad (C) presents again a different donor, being in this case a different BODIPY chromophore. Unlike the acceptor BODIPY, the donor has only one alpha and one meso substituent (Fig. S1b), resulting in a blue-shifted absorption respect to the acceptor. The two BODIPYs are linked via the same substituted cyclohexane bridge used for dyad A, that guarantees a relatively fixed distance between donor and acceptor.

In the following we will describe in detail the results of the static and transient spectroscopic measurements performed for the three dyads. For dyad A the spectroscopic measurements have been carried out in different solvents: chloroform, acetonitrile and benzonitrile. The other samples have been studied in chloroform solution. In the following we present the results obtained in case of chloroform solution; the experimental measurements in the other two solvents are reported in the S.I. section.

3.1. Dyad A

The absorption, emission and excitation spectra of dyad A in chloroform are reported in Fig. 3a. This dyad, which has the same donor and acceptor moieties as dyad D, studied in Ref. [20] but a rigid bridge, presents, as expected, absorption and fluorescence spectra very similar to those of dyad D (see Fig. 2). Three main spectral features are noticeable: the two bands centred around 580 nm and 630 nm represent the contribution of the BODIPY acceptor, while the feature centred around 520 nm is due to the styryl-pyridinium donor. As already found in case of dyad D, the absorption spectrum of the dyad is the sum of the absorption spectra of the two moieties, as shown in Fig. S5a of S.I, indicating poor electronic interaction of the chromophores in the ground state. The fluorescence spectrum of the bichromophore essentially

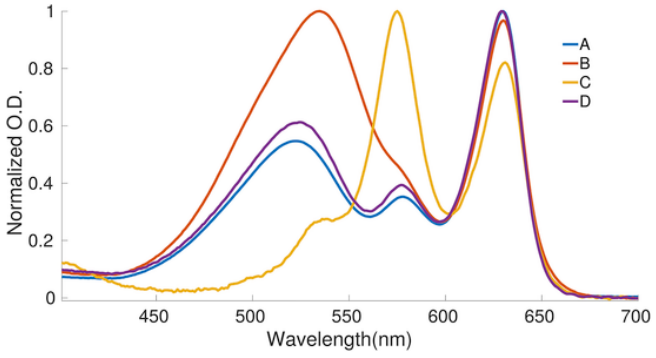

Fig. 2. Linear absorption spectra of the compounds under investigation dissolved in chloroform.

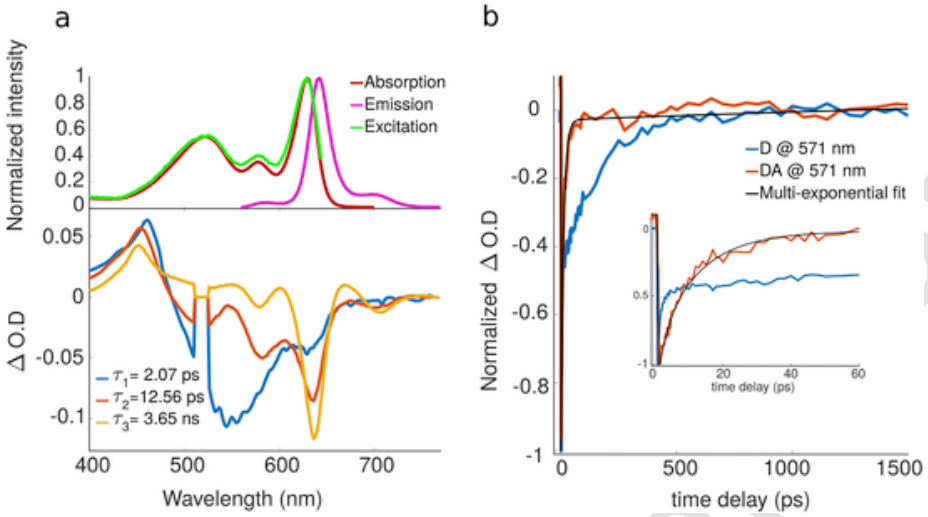

Fig. 3. a) Linear spectra (absorption, emission and excitation) of dyad A in chloroform on topof the EADS obtained by Global analysis performed on transient spectra of dyad A in chloroform. b) Single wavelength kinetics of dyad A and its donor in chloroform taken on the maximum of thedonor bleaching signal, showing ultrafast EET occurring in presence of the acceptor.

corresponds to the emission of the acceptor (Fig. S5b of S.I.), which is an indication of high energy transfer efficiency. The excitation spectrum clearly shows the contribution of the donor to the dyad emission, as expected in presence of energy transfer occurring between the two moieties.

Transient absorption measurements have been carried out by exciting the sample at 530 nm, where the main contribution to the absorption comes from the styryl-pyridinium donor. Recorded transient spectra at different pump-probe delay times are shown in Supplementary Fig. S4. The evolution associated difference spectra (EADS), obtained by performing a Global analysis on the collected time traces, are reported in Fig. 3a. The first spectral component, rising soon after excitation, presents an intense negative feature centred at 550 nm, ascribable to the bleaching of the styryl-pyridinium ground state. A smaller negative shoulder centred at 640 nm corresponds to the bleaching signal of the BODIPY ground state, due to the direct excitation of its absorption band edge. An excited state absorption is also visible on the blue side of the spectrum (positive signal around 450 nm), ascribable to a convolution of signals coming from both the donor and the acceptor, as demonstrated in our previous work [20].

In the two following EADS, respectively rising in $\tau_1 = 2.1$ ps and $\tau_2 = 12.6$ ps, we observe the increase of the BODIPY bleaching/stimulated emission signal and the recovery of the styryl-pyridinium signal, indicating the occurrence of fast and efficient energy transfer. We notice that although the bridge connecting the donor and acceptor is more rigid than that used in dyad D, still the kinetics of energy transfer is bi-exponential, since both the first and second lifetime can be ascribed to this process. The comparison of the kinetic trace at 570 nm, which corresponds to the maximum of the donor bleaching signal, registered in case of the isolated donor and of the dyad, shown in Fig. 3b, evidences a significant increase in ground state recovery rate, due to energy transfer occurring between the two units. The last EADS, which recovers with a time constant $\tau_3 = 3.6$ ns, does not show any residual excitation left on the donor moiety. The time constants retrieved when the measurements are repeated in acetonitrile are very similar to those registered in chloroform. Slightly longer time constants have been found for benzonitrile solution, in agreement with previous results [20]., which can be explained by the larger viscosity of the latter solvent. The EADS obtained in acetonitrile and benzonitrile solution, as well as the single-wavelength kinetics recorded in the different solvents are reported in Fig. S6 of S.I.

3.2. Dyad B

This dyad differs from the one studied in Ref. [20] for the presence of a styryl-pyridinium dimer as donor, that influences both the ground state electronic properties and the excited state dynamics, as described in the following.

The absorption, fluorescence and excitation spectra of the sample are presented in Fig. 4a. Similarly to what observed for dyad A, the bands at 535 nm and 630 nm can be respectively attributed to the double styryl-pyridinium donor and the BODIPY acceptor. Also in this case the absorption spectrum is the sum of the donor and acceptor absorption components, as can be observed in looking at the linear spectra of the different moieties reported in Fig. S7a of S.I.

Differently from the previous sample, here the donor contribution to the absorption spectrum is more pronounced, thus overlapping with the low-wavelength band of the BODIPY absorption, whose shoulder is visible at around 570 nm. Furthermore, similarly to dyad A, a fluorescence Stokes shift of about 10 nm is observed, and the fluorescence spectrum reflects essentially the emission of the acceptor (see Fig. S7b). Also in this case the excitation spectrum indicates that the donor absorption contributes to the emission of the dyad.

The comparison of the absorption spectra of styryl-pyridinium monomer and dimer, reported in Fig. S9 of S.I., indicates negligible changes in the absorption and emission lineshape between the two molecules. However, the presence of a second styryl-pyridinium moiety significantly increases the fluorescence quantum yield (QY) of the dimer respect to the monomer (0.84 for the dimer and 0.1 for the monomer [20], probably due to a conformational restrictions in the dimer compared to the monomer, which has the effect of making the molecular structure more rigid, suppressing some non-radiative decay pathways.

The phenomenon of the QY enhancement in case of the double monomer can be classified as “aggregation induced emission” (AIE), which is the opposite effect to the more common “aggregation-caused quenching” (ACQ) [42]. Dyes in concentrated solutions are indeed characterized by fluorescence quenching, effect that prevents their use as efficient light-harvesting materials. For this reason, our observation makes the styryl-pyridinium an interesting compound for its fluorescence properties.

Transient absorption spectra were recorded also in this case by exciting the he sample was excited with pulsed laser at 532 nm, close

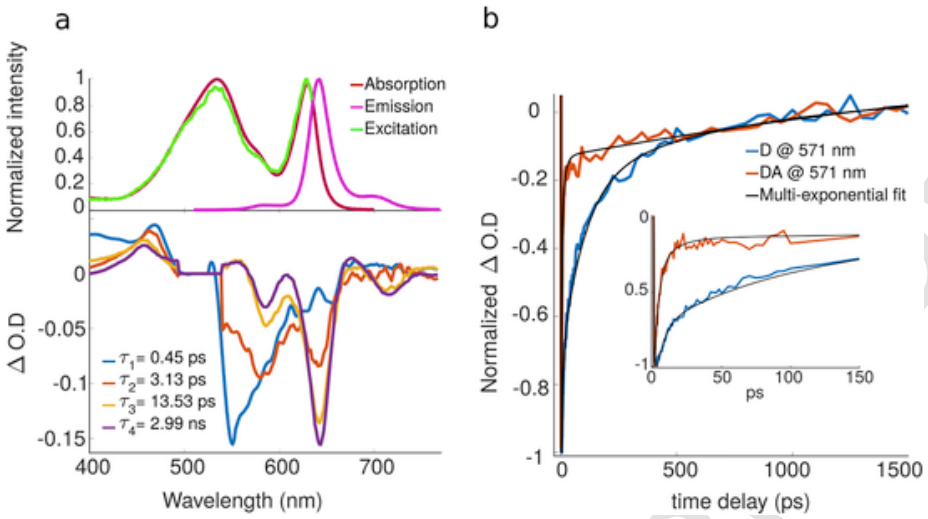

Fig. 4. a) Linear spectra (absorption, emission and excitation) of dyad B in chloroform on topof the EADS obtained by Global analysis performed on transient spectra of dyad B in chloroform. b) Single wavelength kinetics of dyad B and its donor taken on the maximum of the donor bleaching signal, showing ultrafast EET occurring in presence of the acceptor.

to the maximum absorption wavelength of the donor. Recorded transient spectra at several chosen pump-probe delay times are reported in Fig. S8 of S.I. section. The EADS obtained from Global analysis of the transient data in chloroform are presented in Fig. 4a. We found four time-components corresponding to the four time constants. Similarly to dyad A, the first EADS presents the donor ground state bleaching (negative signal centred at 550 nm), together with an excited state absorption on the blue side of the spectrum. In the following three EADS (τ_1= 0.5 ps, τ_2 = 3.1 ps, τ_3 = 13.5 ps), once again we observe the recovery of the donor bleaching and the increase of the BODIPY bleaching/stimulated emission signal (negative band around 635 nm), indicating energy transfer occurring on multiple fast timescales. The ground state of the sample completely recovers with a long time constants of about 3 ns.

To further characterize the electronic properties of the dimeric donor in comparison with the corresponding monomer, we performed a pump-probe measurement on the styryl-pyridinium dimer in chloroform (see S.I. section and the summary Table S2). Within a few picoseconds a dynamic Stokes shift of the stimulated emission is observed, resulting in the formation of a negative double band structure. Furthermore, if compared with the monomer, the excited state lifetime of the styryl-pyridinium dimer appears longer, in agreement with the increased fluorescence quantum yield, as reported in Table S2 and evidenced in Fig. S11 of S.I., where a comparison between the kinetics traces of the monomer styryl-pyridinium and its dimeric form is reported.

Finally, the comparison of the kinetic trace taken on the maximum of the styryl-pyridinium dimer bleaching signal, registered for the isolated donor and the donor-acceptor system, reported in Fig. 4b evidences also in this case an increase of the recovery rate in the presence of the BODIPY acceptor, due to energy transfer.

3.3. Dyad C

In this sample both donor and acceptor are BODIPY chromophores, linked via the same rigid bridge used for dyad A. The absorption spectrum of the dyad, shown in Fig. 5a, corresponds to the sum of the absorptions of the two BODIPY components (see also Fig. S12 of S.I.). The BODIPY acceptor, being the same of the previous samples, is responsible for the absorption band centred at 630 nm. The fluorescence of the dyad substantially corresponds to the acceptor fluorescence with a small residual contribution due to the donor emission.

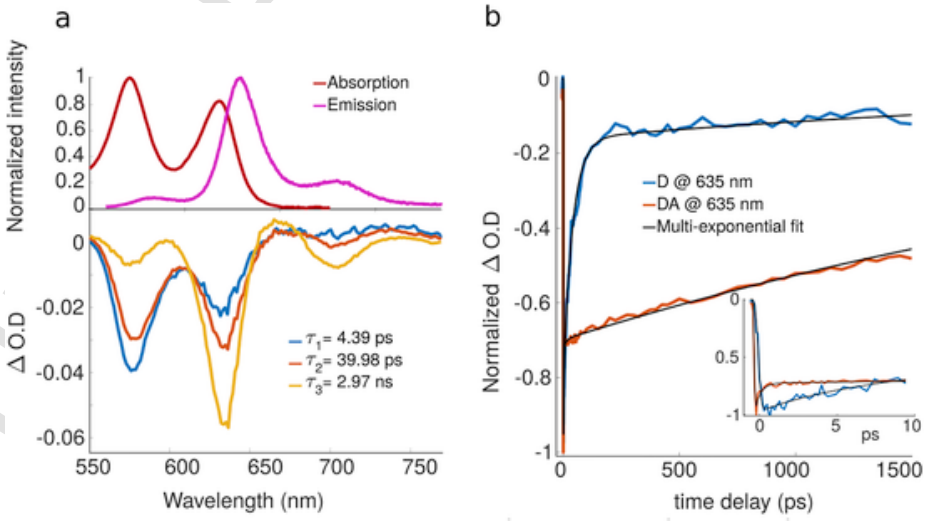

Fig. 5. a) Linear spectra (absorption and emission) of dyad C in chloroform on top of the EADS obtained by Global analysis performed on transient spectra of dyad C in chloroform. b) Singlewavelength kinetics of dyad C and its donor taken on the maximum of the donor bleaching signal, showing ultrafast EET occurring in presence of the acceptor.

Transient absorption measurements were performed in chloroform also in this case by exciting the system at 530 nm, on the blue side of the donor absorption. Experimental TAS spectra at different pump-probe delay times are presented in Supplementary Fig. S13. Global analysis performed on the transient data shows that three kinetic components are sufficient for a satisfactory fit, corresponding to three time-constants. Similarly to the other samples, inspection of the EADS reported in Fig. 5a shows energy transfer occurring on multiple fast timescales (τ_1= 4.4 ps, τ_2 = 40 ps), revealed by the recovery of the negative signal at 550 nm, ascribable to the bleaching/stimulated emission of the BODIPY donor, and the corresponding increase of the acceptor bleaching/stimulated emission at 630 nm. The ground state recovery of the dyad occurs on the nanoseconds timescale (τ_3 = 3 ns).

For further comparison, we also measured the transient absorption spectra of the BODIPY donor in chloroform (Table S2 in S.I.). The fluorescence quantum yield of the BODIPY donor was found to be 0.76. Its transient data are satisfactory fitted using three time constants and the spectral evolution is described by the three EADS reported in Fig. S14a of S.I.. The transient spectrum is characterized by an intense negative signal, centred at 585 nm, due to the convolution of bleaching and stimulated emission, which shows almost no lineshape evolution, and completely recovers on a 3.5 ns timescale. The comparison of the kinetics trace taken on the maximum bleaching signal of the donor, in presence and absence of acceptor, are plotted in Fig. 5b, evidencing also in this case the occurrence of energy transfer, that accelerates the donor recovery rate in the dyad.

4. Discussion

The transient data described above show occurrence of efficient energy transfer in all the investigated compounds, occurring on fast timescales. In the following we discuss differences and similarity of the experimental results among the various samples in order to disentangle the contribution of different molecular factors in determining the overall EET kinetics. The observed electronic behaviours have been interpreted on the basis of the spectral and geometric aspects influencing the dynamics. A summary of the time-constants obtained from global analysis in case of the different samples is presented in Table S2 of S.I.

Considering the average donor-acceptor distance in all the studied dyads and the absence of strong electronic interactions between the chromophores, the Förster model can be safely applied to estimate the energy transfer efficiency. We found it to be close to 100% in all the samples, as it can be observed also by looking at the negligible residual donor fluorescence in the emission spectra (Figs. 3a, 4a and 5a). Table 1 reports a summary of the calculated Förster parameters. In Ref. [20] transient absorption spectroscopy, together with theoretical calculations performed on dyad D (Fig. 1), showed that mobility of the donor-acceptor link allow for coexistence of different conformations in solution, with predominance of certain relative orientations between the two units.

Time-resolved measurements carried out on dyad A, having a rigid linker that keeps donor and acceptor at a fixed distance, show a slower degree of kinetic heterogeneity on the short timescale after excitation compared to dyad D, as it can be observed in the comparison between the collected bleaching kinetics of the two samples (Fig. 6a). Since the absorption spectra of both dyads A and D are the sum of the donor and acceptor components, and their fluorescence is essentially coming from the acceptor, the two units preserve the spectral properties of the isolated monomers. In this picture, the observed multi-exponential energy transfer rate can be explained in terms of geometric factors. In order to quantify the relative distance between donor and acceptor dipole moments, we used an energy transfer model based on the Förster equation, following the procedure described in Refs. [20,43]. From Förster's theory [44], energy transfer rate K_{EET} is given by

$$K_{EET} = \frac{9000 ln\,(10)\, k^2_{\varphi D} J}{128 \pi^5 n^4 N_{A\tau D} R^6} \quad (2)$$

Where the orientation factor k^2 can be approximated to a value of 2/3 (assuming random orientation), φ_D and τ_D are the fluorescence

Table 1
Summary of the Förster Parameters for EET estimated from TAS measurements. ET is the EET rate, J is the Förster spectral overlap, is described in eq. (6) and R is the donor-acceptor distance..

	K_{EET} (ps^{-1})	J $(M^{-1}cm^{-1}nm^4)$	R_0 ()	R ()	E (%)
dyad A	$4.8 \cdot 10^{-1}$	$7.65\ 10^{15}$	46.65	17.16	99.75
	$7.9 \cdot 10^{-2}$			23.19	98.51
dyad B	2.5	$7.93\ 10^{15}$	66.96	18.73	99.95
	$3.2 \cdot 10^{-1}$			26.35	99.63
	$7.4 \cdot 10^{-2}$			36.67	98.41
dyad C	$2.3 \cdot 10^{-1}$	$7.38\ 10^{15}$	65.06	21.37	99.87
	$2.5 \cdot 10^{-2}$			30.88	98.87
dyad D	1.7	$1.02\ 10^{16}$	48.98	14.66	99.93
	$1.6 \cdot 10^{-1}$			21.63	99.26

Fig. 6

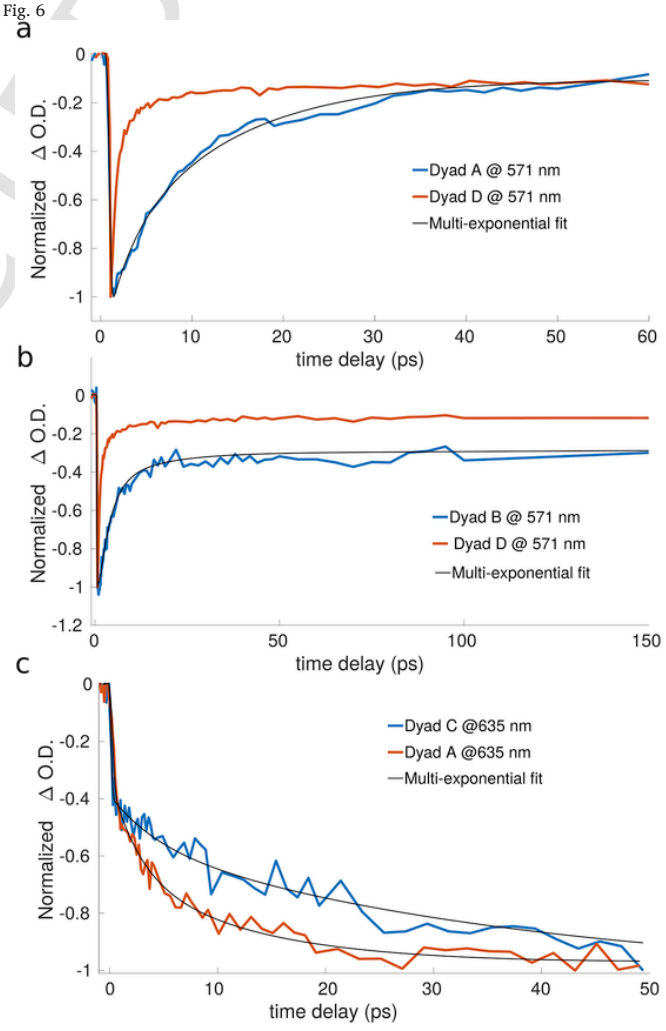

a) Single wavelength kinetics taken at the maximum of the donor bleaching signal in case of dyads A and D. b) Single wavelength kinetics taken at the maximum of the donor bleaching signal in case of dyad B and D. c) Single wavelength kinetics taken at the maximum of the acceptor bleaching signal in case of dyad C and B.

QY and lifetime of the donor (experimentally determined), n is the refractive index of the solvent, N_A is Avogadro's number, R is the donor-acceptor distance and J is the spectral overlap integral, defined as:

$$J = \int_0^\infty \frac{F_D(\nu) \in A(\nu)\, d\nu}{\nu^4} \tag{3}$$

Here F_D is the normalized fluorescence of the donor and $\in_A$ is the absorption coefficient of the acceptor. The value of $\in_A$ for the BODIPY acceptor was taken from Ref. [45].

We report all the parameters used and the overlap integral calculations in S.I. section. For any energy transfer rate estimated from transient absorption measurements, it is possible to calculate the average distance R between the dipole moments by inverting eq. (2):

$$R = \sqrt[6]{\frac{9000 ln(10)\, k^2_{\varphi D} J}{128\pi^5 n^4 N_{A\tau D} K_{EET}}} \tag{4}$$

Finally, is it straightforward to calculate the energy transfer efficiency:

$$E = \frac{R_0^6}{R^6 \left| + R_0^6\right.} \tag{5}$$

where

$$R_0 = 0.211\left(\frac{k^2_{\varphi D} J}{n^4}\right)^{\frac{1}{6}} \tag{6}$$

Using the experimental data from Ref. [20] relative to dyad D, we estimate that 70% of energy transfer occurs within a sub-picoseconds timescale (τ_1= 0.6 ps in chloroform), corresponding to a donor-acceptor distance R_1 = 14 Å. The residual energy transfer, described by the time-constant = $\tau_2$6.2 ps, results in a distance R_2 = 21 Å.

The same model is applied to dyad A, where energy transfer dynamics follows a double-exponential trend with time constants $\tau_1 = 2.1$ ps and $\tau_2 = 12.6$ ps, corresponding approximately to 55% and 45% of energy exchange, respectively. By inserting these two time constants in eq. (4), we get distances $R_1 = 17$ Å and $R_2 = 23$ Å. The distance between donor and acceptor in dyad D is thus smaller respect to dyad A, which is expected due to the fact that the rigid linker of the latter molecule does not allow for maximization of the dipole coupling, occurring when reducing the relative angle between the styryl-pyridinium and the BODIPY. Furthermore, the linkers in A and D have different lengths: the estimated difference from the molecular structure is on the order of 4 Å.

Analogously dyad B can be compared to dyad D to evidence the effects of introducing a styryl-pyridinium group on the donor moiety, leaving the same BODIPY acceptor and the same linker used in dyad D. Also in this case the energy transfer rate appears slower than for dyad D, as it can be observed by the comparison shown in Fig. 6b. Here different factors could play a role in the energy transfer dynamics: the dimer styryl-pyridinium donor has indeed a much higher QY respect to the monomer form, and a larger time-constant for ground state recovery after excitation (see stationary and transient characterization in S.I.). As a consequence, the overlap integral is also substantially larger than for dyad D. This factors are supposed to increase the energy transfer rate as calculated in eq. (2). However, geometrical effects due to the steric hindrance of the dimer styryl-pyridinium group reduce importantly the energy transfer efficiency. By applying eq. (4) we found indeed $R_1 = 19$ Å, $R_2 = 26$ Å and $R_3 = 37$ Å, associated to time-constant of $\tau_1 = 0.4$ ps, $\tau_2 = 3.1$ ps and $\tau_3 = 13.5$ ps, which in turn contributes for 54%, 33% and 12% of energy transfer, respectively.

In order to address the influence of the dimer styryl-pyridinium on the energy transfer efficiency and to make an accurate comparison with the case of the monomer styryl-pyridinium donor (dyad D), we performed a theoretical optimization of several donor-acceptor conformations at the M062X/6-311G(d)/PCM level. We selected the lowest energy conformations and we computed free energies and total couplings between the two donor monomers and between each styryl-pyridinium and the BODYPI acceptor. In the calculations we assumed that the two styryl-pyridinium moieties of the donor are independent, and EET occur between a single donor monomer and the acceptor with the same probability. This assumption is motivated by the observation that the absorption spectra of the single and double styryl-pyridinium donors are almost the same. For all TDDFT calculations, the solvents effects were included in the linear response formalism.

In agreement with the experimentally observed excited state dynamics, that shows a multi-exponential behaviour of the energy transfer, we found several stable configurations of the dye which are very similar in energy but with different angles of orientation between donor and acceptor. Calculated EET rates are in agreement with experimental ones in case of three conformers (Conformers number 19, number 5 and number 11, see Table 2). The identified conformers are characterized by a large donor-acceptor distance (open conformations), proving that the geometric arrangement of the two moieties is influenced by the steric hindrance of the dimer styryl-pyridinium donor. Table 2 shows the computed EET parameters and the geometrical parameters associated to the optimized configurations (donor-acceptor centre of mass distances and angles of orientations, as defined in Fig. 7. We have highlighted with the same color in the two tables the experimental EET rates K_{EET} in Table 1 that have been ascribed to theoretical ones in Table 2. The two fast component (highlighted in green and red in Tables 1 and 2) are characterized by strong coupling and short donor-acceptor distances, as expected. The energy transfer is driven maily by coupling with one of the two donor moieties, indiceted as D2 in Table 2. On the other hand, the comparison between calculated and experimental EET rates shows that for the longer time component energy transfer also involves the other donor moiety (D1 in Table 2), that is slightly more distant and less coupled with the acceptor.

Table 2
Computed and EET parameters of different optimized configurations of Dyad B..

Conformer	Angles ($\beta/\gamma/\alpha$)	Population	Donor	K_{EET} (ps^{-1})	EET time (ps)	R ()
19	−55 / −175 / 51	100	D1	$5.5 \cdot 10^{-3}$	180	18.5
			D2	$3.3 \cdot 10^{-1}$	3.9	15.7
5	−68 / −154 / 66	22	D1	$5.8 \cdot 10^{-2}$	17	17.5
			D2	$1.7 \cdot 10^{-1}$	6.0	16.4
11	−72 / −173 / 45	7	D1	$1.21 \cdot 10^{-2}$	81	19.5
			D2	3.6	0.28	11.6

Fig. 7

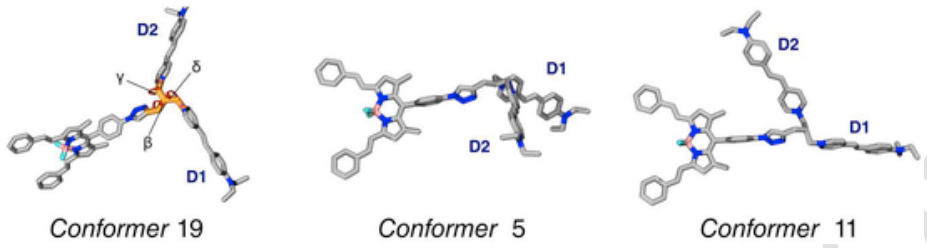

a) Chemical structure of dyad B showing the three conformations considered in Table 2, characterized by different relative orientations between the three units (angles β,γ,α).

In the supporting information section S5 we report a comparison between computed and experimental donor-acceptor energy couplings in case of dyad B (Table S3), which are in very good agreement, and a summary of EET parameters of dyads B (for the three conformers 19, 5 and 11) and D (from Ref. [20], see Table S4). The computed EET time-constants are very similar between the two dyads, showing only a slight acceleration of the energy transfer in case of dyad A. This result is in agreement with the experimental EET rates summarized in Table 1. However, as it can be observed from the kinetic traces in Fig. 6b, the kinetic trace associated to dyad B appears to decay faster. This observation can be explained by considering that in dyad D EET occurs mainly at fast timescales ($\tau = 6.2$ ps), while in case of dyad B two close time constants (3.1 ps and 13.5p s) are found to contribute to the EET. This two timescales are ascribed to conformer *19* and *11* (see Table 1), which have indeed similar relative donor-acceptor orientations (Fig. 7).

Finally, we applied the Förster theory also to dyad C, whose kinetic trace at 579 nm is compared to that of dyad D taken at the same wavelength in Fig. 6c. These two samples differs substantially for the donor moieties, being in one case a monomer styryl-pyridinium group and in the other a substituted BODIPY (Fig. 1) respectively. The donor acceptor link in both samples is the rigid cyclohexane with aliphatic chains. The QY of the BODIPY donor (QY = 0.76) is quite larger than that of the monomer styryl-pyridinium present in dyad D. However, the excited state lifetime of the donor alone is much longer than the single styryl-pyridinium one (see Fig. S15 of S.I.). When all the experimental factors have been correctly inserted in eq. (4), we obtain donor-acceptor distance $R_1 = 21$ Å and $R_2 = 31$ Å (corresponding to $\tau_1 = 4.4$ ps and $\tau_2 = 40$ ps), which contribute to the 30% and 70% of energy transfer, respectively.

All the consideration reported in this section can be summarized by looking at Fig. 6, which presents comparisons between ultrafast dynamics of analogous compounds, taken at wavelength of interest. In panel a) we show kinetic traces of dyad A and D recorded at wavelength corresponding to the maximum of the donor bleaching signal. The two compounds differs only in the nature of the donor-acceptor link, whose rigidity slows down the EET in case of dyad A. In panel b) the comparison between kinetic traces of dyad B and D collected on the maximum bleaching signal of the donor shows differences due to the presence of the dimer styryl-pyridinium donor, as discussed above. Finally, in panel c) kinetic traces recorded on the maximum bleaching signal of the acceptor are reported in case of dyad C and A, demonstrating the influence of different donors on the excited state dynamics.

5. Conclusions

We have investigated the effect of chemical structure modifications on the energy transfer dynamics in donor-acceptor pairs, by combining time-resolved spectroscopy and theoretical calculations performed at DFT level. Our study focuses on the nature of the donor and on the rigidity of the donor-acceptor linker. All the compounds investigated have shown fast and extremely efficient energy transfer (up to 99%), because the chemical and spectroscopic properties of the moieties allow stable configurations characterized by short donor-acceptor distances large spectral overlap. The presence of a rigid bridge between the BODIPY acceptor and the single styryl-pyridinium donor slows down the EET process of the dyad with respect to the case of the mobile linker studied in Ref. [20], which can be explain by considering that increase of rigidity forbids a number of relative orientations between donor and acceptor which could favour EET. The introduction of a dimer styryl-pyridinium donor, characterized by high QY due to the AIE effect, linked to the acceptor by means of a mobile bridge, influence the time-behaviour of the system by introducing an additional fast contribution to EET on the picoseconds timescale, due to steric hindrance effects. In this case we found that EET presents multi-exponential kinetics, in agreement with theoretical modelling of energetic couplings and EET rates performed on optimized geometries of the dyads in solution. We were able to assign the experimental EET time-constant to calculated ones with great accuracy, and to ascribe the time contributions to different structural configurations of the compound, described by different calculated dihedral angles between each donor and the acceptor. The presence of three units (two styryl-pyridinium moiety and the BODIPY acceptor) allows increased mobility of the system, and efficient EET can occur because of the small distances between one of the two donor monomers and the acceptor, as it is can be observed in the stable configurations of Fig. 7. Donor acceptor distances obtained by modelling time-resolved experimental data with Förster equation were also in very good agreement. Finally, in the last chemical modification introduced, a BODIPY dye was used as donor. No substantial differences were observed with respect to the other samples studied. Our results highlight the importance of spatial effects, which can have a significant impact on the electronic behaviour of a bichromophoric compound on ultrafast timescales. Our experimental and theoretical data demonstrate that in case of the studied systems can prevail over other effects due to chemical and electronic properties of the conformers.

Acknowledgements

This work was supported by the European Union, through the Horizon 2020 Research and Innovation Programme (RIA "Laserlab-Europe", n. 654148).

The authors acknowledge the support and the use of resources of Instruct-ERIC, a Landmark ESFRI project, and specifically the CERM/CIRMMP Italy Centre.

Appendix A. Supplementary data

Supplementary data to this article can be found online at https://doi.org/10.1016/j.dyepig.2019.108010.

Uncited references

[46].

References

[1] Y-C Cheng, GR Fleming. Dynamics of light harvesting in photosynthesis. Annu Rev Phys Chem 2009;60(1):241–262.

[2] V Balzani, A Credi, M Venturi. Photochemical conversion of solar energy. Chem Sus Chem 2008;1(1–2):26–58.
[3] D Gust, T Moore, A Moore. Solar fuels via artificial photosynthesis. Acc Chem Res 2009;42(12):1890–1898.
[4] J Barber. Photosynthetic energy conversion: natural and artificial. Chem Soc Rev 2009;38(1):185–196.
[5] GD Scholes, GR Fleming, A Olaya-Castro, R Van Grondelle. Lessons from nature about solar light harvesting. Nat Chem 2011;3(10):763–774.
[6] I McConnell, G Li, GW Brudvig. Energy conversion in natural and artificial photosynthesis. Chem Biol 2010;17(5):434–447.
[7] S Cicchi, P Fabbrizzi, G Ghini, A Brandi, P Foggi, A Marcelli, et al. Pyrene-excimers-based antenna systems. Chem Eur J 2009;15(3):754–764.
[8] O Kühn, V Sundström. "Pump–probe spectroscopy of dissipative energy transfer dynamics in photosynthetic antenna complexes: a density matrix approach. J Chem Phys 1997;107(11):4154–4164.
[9] AR Holzwarth, G Schatz, H Brock, E Bittersmann. Energy transfer and charge separation kinetics in photosystem I: Part 1: picosecond transient absorption and fluorescence study of cyanobacterial photosystem I particles. Biophys J 1993;64(6):1813–1826.
[10] R Croce, MG Müller, R Bassi, AR Holzwarth. Carotenoid-to-chlorophyll energy transfer in recombinant major light-harvesting complex (LHCII) of higher plants. I. Femtosecond transient absorption measurements. Biophys J 2001;80(2):901–915.
[11] A Iagatti, S Doria, A Marcelli, N Angelini, S Notarantonio, AM Paoletti, et al. Photophysical processes occurring in a zn-phthalocyanine in ethanol solution and on tio2 nanostructures. J Phys Chem C 2015;119(35):20256–20264.
[12] I Tosi, B Bardi, M Ambrosetti, E Domenichini, A Iagatti, L Baldini, et al. Investigation of electronic energy transfer in a bodipy-decorated calix[4]arene. Dyes Pigments 2019;171:107652.
[13] O Maier, V Oberle, D Hoekstra. Fluorescent lipid probes-some properties and applications (a Review).Pdf. Chem Phys Lipids 2002;116:3–18.
[14] P Majumdar, X Yuan, S Li, B Le Guennic, J Ma, C Zhang, et al. Cyclometalated Ir(iii) complexes with styryl-BODIPY ligands showing near IR absorption/emission: preparation, study of photophysical properties and application as photodynamic/luminescence imaging materials. J Mater Chem B 2014;2(19):2838–2854.
[15] I Mikhalyov, N Gretskaya, F Bergström, LB Johansson. Electronic ground and excited state properties of dipyrromethene boron difluoride (BODIPY): dimers with application to biosciences. Phys Chem Chem Phys 2002;4(22):5663–5670.
[16] J-S Lee, N-Y Kang, YK Kim, A Samanta, S Feng, HK Kim, et al. Synthesis of a BODIPY library and its application to the development of live cell glucagon imaging probe. J Am Chem Soc 2009;131:10077–10082.
[17] S Erten-Ela, MD Yilmaz, B Icli, Y Dede, S Icli, EU Akkaya. A panchromatic boradiazaindacene (BODIPY) sensitizer for dye-sensitized solar cells. Org Lett 2008;10(15):3299–3302.
[18] S Kolemen, OA Bozdemir, Y Cakmak, G Barin, S Erten-Ela, M Marszalek, et al. Optimization of distyryl-Bodipy chromophores for efficient panchromatic sensitization in dye sensitized solar cells. Chem Sci 2011;2(5):949–954.
[19] H Anders, G Boschloo, L Sun, L Kloo, H Pettersson. Dye-sensitized solar cells. Chem Rev 2010;110:6595–6663.
[20] M Di Donato, A Iagatti, A Lapini, P Foggi, S Cicchi, L Lascialfari, et al. Combined experimental and theoretical study of efficient and ultrafast energy transfer in a molecular dyad. J Phys Chem C 2014;118(41):23476–23486.
[21] T Deligeorgiev, A Vasilev, S Kaloyanova, JJ Vaquero. Styryl dyes - synthesis and applications during the last 15 years. Color Technol 2010;126(2):55–80.
[22] A Mishra, RK Behera, PK Behera, BK Mishra, GB Behera. Cyanines during the 1990s: a review. Chem Rev 2000;100(6):1973–2011.
[23] J Saltiel, DWL Chang, ED Megarity, AD Rousseau, PT Shannon, B Thomas, et al. The triplet state in stilbene cis-trans photoisomerization. Pure Appl Chem 1975;41(4):559–579.
[24] ES Cockburn, RS Davidson, JE Pratt. The photocrosslinking of styrylpyridinium salts via a [2 + 2]-cycloaddition reaction. J Photochem Photobiol A Chem 1996;94(1):83–88.
[25] IA Al-Ansari. Interaction of solvent with the ground and excited state of 2- and 4-[4-(dimethylamino)styryl]-1-alkylpyridinium iodides: an absorption and fluorescence study. Bull Soc Chim Fr 1997;134(6):593–599.
[26] K Takagi, Y Ogata. Visible-light-sensitized cis-trans isomerization of N-methyl-4-(.beta.styryl)pyridinium ions. J Org Chem 1982;47(8):1409–1412.
[27] FH Quina, DG Whitten. "Photochemical reactions in organized monolayer assemblies. 4. Photodimerization, photoisomerization, and excimer formation with surfactant olefins and dienes in monolayer assemblies, crystals, and Micelles1'2. J Am Chem Soc 1977;99(3):877–883.
[28] E Ragnoni, M Di Donato, A Iagatti, A Lapini, R Righini. "Mechanism of the intramolecular charge transfer state formation in all-trans-β-apo-8'-carotenal: influence of solvent polarity and polarizability. J Phys Chem B 2015;119(2):420–432.
[29] IH van Stokkum, DS Larsen, R van Grondelle. Global and target analysis of time- resolved spectra. Biochim Biophys Acta Bioenerg 2004;1657(2):82–104.
[30] A Mabied, S Nozawa, M Hoshino, A Tomita, T Sato, S Ichi Adachi. Application of singular value decomposition analysis to time-dependent powder diffraction data of an in-situ photodimerization reaction. J Synchrotron Radiat 2014;21:554–560.
[31] J Snellenburg, S Laptenok, R Seger, K M Mullen, I Van Stokkum, " Glotaran. A java-based graphical user interface for the r package timp. J Stat Softw 2012;49:1–22.
[32] K Mullen, I van Stokkum. Timp: an r package for modeling multi-way spectroscopic measurements. J Stat Softw 2007;18(3).
[33] C Azarias, L Cupellini, A Belhboub, B Mennucci, D Jacquemin. Modelling excitation energy transfer in covalently linked molecular dyads containing a bodipy unit and a macrocycle. Phys Chem Chem Phys 2018;20:1993–2008.
[34] C Azarias, R Russo, L Cupellini, B Mennucci, D Jacquemin. Modeling excitation energy transfer in multi-bodipy architectures. Phys Chem Chem Phys 2017;19:6443–6453.
[35] C-P Hsu, GR Fleming, M Head-Gordon, T Head-Gordon. Excitation energy transfer in condensed media. J Chem Phys feb 2001;114:3065–3072.
[36] MF Iozzi, B Mennucci, J Tomasi, R Cammi. Excitation energy transfer (EET) between molecules in condensed matter: a novel application of the polarizable continuum model (PCM). J Chem Phys apr 2004;120:7029–7040.
[37] J Tomasi, B Mennucci, R Cammi. Quantum mechanical continuum solvation models. Chem Rev aug 2005;105:2999–3094.
[38] Y Zhao, DG Truhlar. The m06 suite of density functionals for main group thermo-chemistry, thermochemical kinetics, noncovalent interactions, excited states, and transition elements: two new functionals and systematic testing of four m06 functionals and 12 other functionals. Theor Chem Acc jan 2008;119. 525–525.
[39] T Yanai, DP Tew, NC Handy. "A new hybrid exchange–correlation functional using the coulomb-attenuating method (CAM-b3lyp). Chem Phys Lett jul 2004;393:51–57.
[40] AV Marenich, CJ Cramer, DG Truhlar. Universal solvation model based on solute electron density and on a continuum model of the solvent defined by the bulk dielectric constant and atomic surface tensions. J Phys Chem B may 2009;113:6378–6396.
[41] GD Scholes. Long-range resonance energy transfer in molecular systems. Annu Rev Phys Chem jan 2003;54:57–87.
[42] Y Hong, JWY Lam, BZ Tang. Aggregation-induced emission. Chem Soc Rev 2011;40:5361–5388.
[43] PL Gentili, M Mugnai, L Bussotti, R Righini, P Foggi, S Cicchi, et al. The ultrafast energy transfer process in naphtole-nitrobenzofurazan bichromophoric molecular systems. A study by femtosecond UV-vis pump-probe spectroscopy. J Photochem Photobiol A Chem 2007;187(2–3):209–221.
[44] T Förster. Transfer mechanisms of electronic excitation energy. Radiat Res Suppl 1960;2:326.
[45] S Fedeli, P Paoli, A Brandi, L Venturini, G Giambastiani, G Tuci, et al. Azido-substituted BODIPY dyes for the production of fluorescent carbon nanotubes. Chem Eur J 2015;21(43):15349–15353.
[46] U Resch-Genger, K Rurack. Determination of the photoluminescence quantum yield of dilute dye solutions (iupac technical report). Pure Appl Chem 2013;85:2005–2013.